Supplementary Materials

Supplementary materials Table 1: *Lophelia pertusa* occurrence locations with associated water chemistry in the Southern California Bight. Distinct occurrences were classified by 1) a minimum survey time of 3 minutes since last occurrence or 2) by an occurrence separated by distinctly different substrate. Occurrence column includes characterization of reef-building (RB), patchy aggregations (PA), sparse live patches (SL), or rubble only (RO). Depth is noted as maximum and minimum for occurrences at each site. Temperature (C), salinity (psu), and oxygen (µmol/kg) are mean values (2007-2015) from deepest and shallowest occurrence respectively. These values were extracted from the nearest California Cooperative Oceanic Fisheries Investigations station. Mean aragonite saturation, dissolved inorganic carbon (µmol/kg), $pH_{(T)}$, and total alkalinity (µmol/kg), (deepest then shallowest), were derived from empirical algorithms (see Methods), which were validated with conductivity-temperature-depth cast bottle samples in 2015 (Supplementary Materials Figure 1). All coral locations are available at https://deepseacoraldata.noaa.gov/. Water chemistry data is available at http://calcofi.org/. 'Sampling sites' represent values at time of *L. pertusa* collection.

Site	Year	Latitude, Longitude	Occurrences	Depth m	Temp in °C	Salinity in PSU	Oxygen in µmol/kg	$\Omega_{(arag)}$	Dissolved Inorganic Carbon in µmol/kg	$pH_{(T)}$	Total Alkalinity in µmol/kg
109 Seamount	2004	32.558 -119.494	10 (1 RB; 1 PA; 7 SL; 1 RO)	224 160	8.3 9.0	34.12 33.98	73.6 102.2	0.78 0.90	2239.6 2209.1	7.64 7.69	2280.7 2264.5
Cortes Spawning Grounds	2005	32.583 -119.194	1 RO	209	8.4	34.1	79.4	0.81	2233.5	7.65	2277.7
9 Mile Bank	2005	32.621 -117.400	1 SL	170	9.7	34.07	83.0	0.91	2211.2	7.68	2266.8
Potato Bank	2005	33.265 -119.842	1 SL	88	10.0	33.68	148.1	1.17	2152.4	7.79	2237.7
San Clemente Island	2005	32.818 -118.341	2 SL	159 123	9.3 9.8	33.99 33.82	106.7 128.6	0.96 1.07	2200.5 2172.5	7.71 7.75	2262.9 2247.6
57 Fathom Reef	2005	32.799 -118.525	1 SL	109	10.2	33.79	128.3	1.07	2169.6	7.75	2244.7

Santa Barbara Island	2007	33.468 -119.107	2 RB	88 82	10.1 10.2	33.74 33.71	133.0 138.3	1.09 1.12	2164.7 2159.2	7.75 7.76	2242.3 2240
81 Fathom Bank	2007	32.719 -118.406	5 (3 SL; 1 SD; 1 RO)	223 152	8.7 9.4	34.15 33.96	73.2 109.9	0.82 0.97	2234.6 2196.1	7.65 7.72	2280.6 2260.3
118 Bank	2007	33.073 -119.640	2 SL	253 248	8.0 8.0	34.16 34.16	58.7 60.3	0.74 0.75	2251.8 2250.2	7.62 7.62	2287.5 2286.7
107 Bank	2007	33.048 -119.608	2 SL	239 198	8.1 8.5	34.15 34.09	63.9 81.2	0.76 0.82	2246.9 2230.1	7.63 7.66	2285.1 2277.1
Del Mar Steeples	2008	32.935 -117.315	2 SL	84 75	10.8 11.0	33.69 33.63	137.8 148.5	1.21 1.28	2146.5 2135.4	7.78 7.80	2237.0 2233.3
Kidney Bank	2008	33.165 -118.411	2 SL	238 139	8.8 9.6	34.17 33.95	65.8 105.0	0.81 0.98	2238.3 2195.2	7.64 7.71	2281.5 2258.6
Mission Beach Reef	2011	32.779 -117.381	1 SL	170	9.7	34.06	83.4	0.92	2211.0	7.68	2266.6
Osborne Bank	2012	33.362 -119.044	3 (2 RB; 1 SL)	191 81	8.9 10.6	34.14 33.63	72.5 152.8	0.82 1.24	2233.0 2140.1	7.65 7.80	2277.8 2234.0
Hidden Reef	2012	33.708 -119.134	1 RB; 11 SL	199 154	9.0 9.4	34.13 34.00	73.1 96.4	0.84 0.94	2230.0 2204.4	7.65 7.70	2277.2 2263.6
Lasuen Knoll	2012	33.400 -117.998	4 SL	147 117	9.8 10.1	33.98 33.85	100.1 119.9	0.98 1.08	2196.1 2174.1	7.71 7.74	2259.8 2248.9
Santa Catalina Island	2012	33.466 -118.624	7 (1 PA; 6 SL)	178 68	9.2 11.0	34.08 33.56	84.2 167.7	0.88 1.35	2218.5 2122.8	7.67 7.84	2271.0 2229.4
43 Fathom Bank	2012	32.653 -117.974	4 (1 RB; 2 SL; 1 RO)	236 100	8.8 10.5	34.17 33.71	66.3 139.9	0.81 1.19	2237.5 2151.2	7.64 7.78	2281.0 2239.1
Cortes Bank	2012	32.549 -119.334	7 (2 RB; 5 SL)	213 92	8.4 10.2	34.10 33.62	77.7 155.5	0.80 1.17	2235.3 2147.2	7.65 7.79	2278.6 2233.8
Tanner Bank	2012	32.699 -119.115	4 SL	179 84	9.0 10.3	34.08 33.64	85.3 151.7	0.85 1.17	2223.4 2148.4	7.67 7.78	2272.9 2234.8
Cherry Bank	2012	32.891 -119.400	9 (1 RB; 3 PA, 5 SL)	241 93	8.1 10.1	34.14 33.63	65.7 154.3	0.76 1.16	2246.4 2148.4	7.63 7.79	2283.8 2234.2
San Nicolas Island	2012	33.301 -119.513	8 (1 PA; 7 SL)	242 79	8.5 10.3	34.20 33.69	54.5 140.8	0.75 1.14	2251.1 2155.9	7.61 7.77	2286.7 2238.7
The Footprint-East Ridge	2015	33.955 -119.465	8 (1 PA, 7 SL)	265 175	8.4 9.2	34.21 34.07	50.6 84.8	0.74 0.89	2253.9 2217.3	7.61 7.68	2288.9 2270.3

San Miguel Pass	2015	34.091 -120.244	1 RB	78	10.2	33.80	121.3	1.09	2170.8	7.75	2247.1
The Footprint-Mid Ridge	2015	33.959 -119.475	20 (1 RB; 7 PA; 10 SL; 2 RO)	196 149	9.0 9.5	34.13 33.98	75.1 99.9	0.85 0.95	2228.1 2201.0	7.66 7.70	2276.3 2261.8
South Santa Rosa	2015	33.857 -119.990	1 PA	66	10.6	33.71	148.1	1.24	2146.0	7.80	2238.9
Anacapa Deep Ridge	2015	33.979 -119.410	1 SL	285	8.2	34.22	45.8	0.72	2259.0	7.60	2291.4
Piggy Bank	2015	33.920 -119.477	37 (10 PA; 24 SL; 3 RO)	313 276	8.1 8.3	34.25 34.22	38.4 47.9	0.70 0.73	2266.5 2256.7	7.59 7.61	2295.3 2290.2
The Footprint-West Ridge	2015	33.963 -119.489	12 (2 RB; 7 PA; 3 SL)	115 90	9.9 10.3	33.84 33.70	120.3 142.0	1.05 1.17	2176.5 2152.8	7.74 7.78	2248.9 2238.7
Sampling sites											
Piggy Bank	2010	33.919 -119.473	N/A	288	8.2	34.22	45.1	0.72	2259.8	7.60	2291.7
The Footprint-East Ridge	2014	33.955 -119.462	SL	248	8.5	34.20	54.9	0.76	2249.0	7.62	2286.5
The Footprint-West Ridge	2014	33.964 -119.489	PA	102	10.1	33.77	129.6	1.10	2166.2	7.76	2244.1
The Footprint-East Ridge	2014	33.957 -119.469	SL	175	9.2	34.07	84.8	0.89	2217.3	7.68	2270.35
Piggy Bank	2014	33.918 -119.473	PA	301	8.1	34.24	40.8	0.71	2263.9	7.60	2293.8
Piggy Bank	2015	33.919 -119.472	PA	293	8.2	34.23	43.3	0.72	2261.4	7.60	2292.6
The Footprint-Mid Ridge	2015	33.959 -119.475	SL	168	9.3	34.05	87.9	0.90	2213.4	7.68	2268.3
The Footprint-West Ridge	2015	33.964 -119.489	RB	92	10.3	33.72	138.7	1.15	2156.1	7.78	2240.0

The Footprint-Mid Ridge	2015	33.959 -119.476	PA	174	9.2	34.07	85.3	0.89	2216.8	7.68	2270.2
Piggy Bank	2015	33.919 -119.472	PA	291	8.2	34.23	44.3	0.72	2260.4	7.60	2292.0

Supplementary materials Figure 1: Bathymetric map of *Lophelia pertusa* occurrences in the Southern California Bight. Red and black circles represent sites where *L. pertusa* was present and absent, respectively. The inset shows two sites of particularly high abundance, Piggy Bank and Footprint in the Channel Islands National Marine Sanctuary.

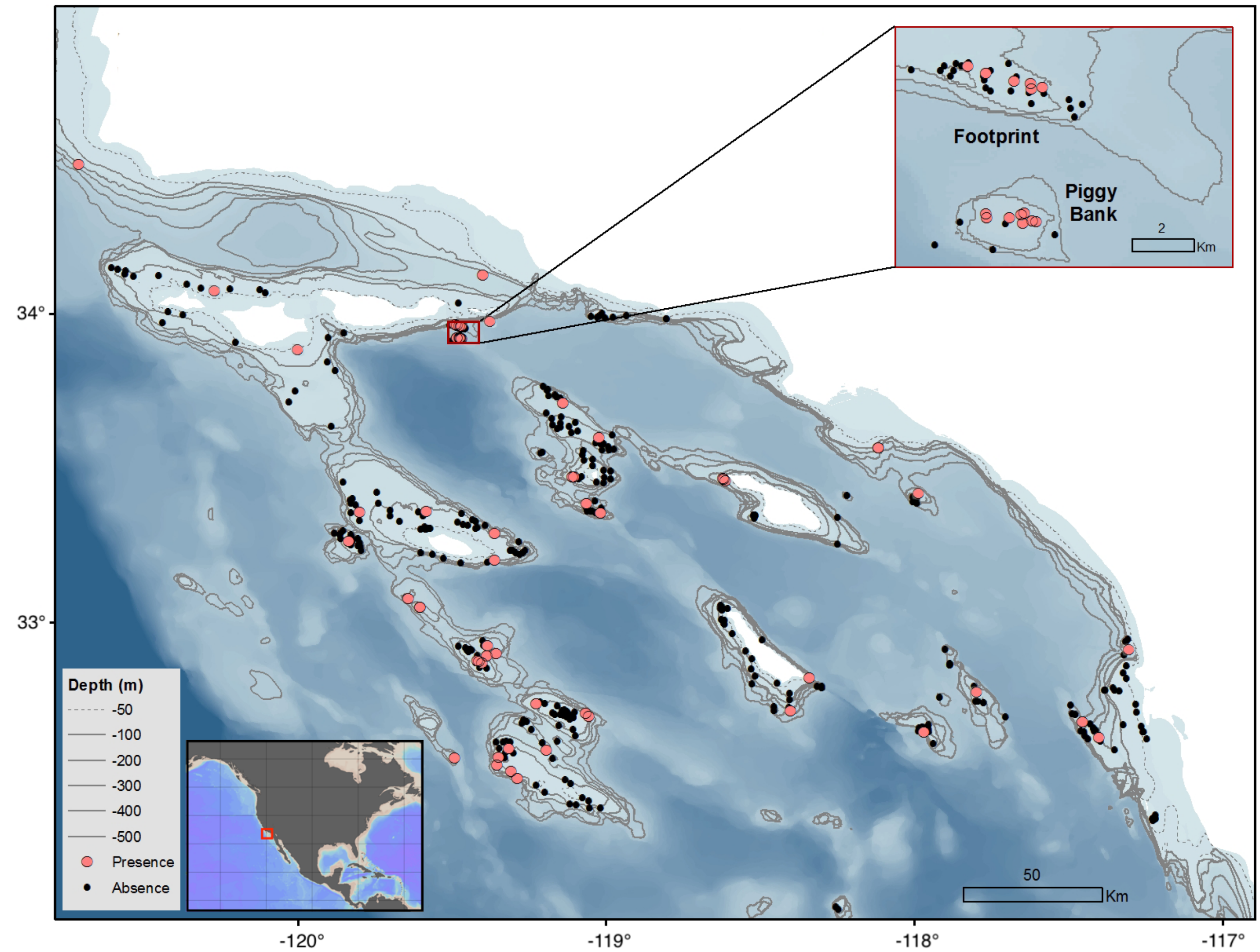

Supplementary materials Figure 2: Aragonite saturation profile in the Channel Islands National Marine Sanctuary. Box plots represent aragonite saturation values derived from an algorithm (see Methods) using California Cooperative Oceanic Fisheries Investigation data from 2007-2015. The boxplots show median values, first and third quartiles, minimum and maximum values and outliers. Red points are from conductivity-temperature-depth (CTD) cast bottle samples collected in June 2010, March 2015 and August 2015. Blue dots represent depths of *Lophelia pertusa* occurrences at their respective median aragonite saturation values.

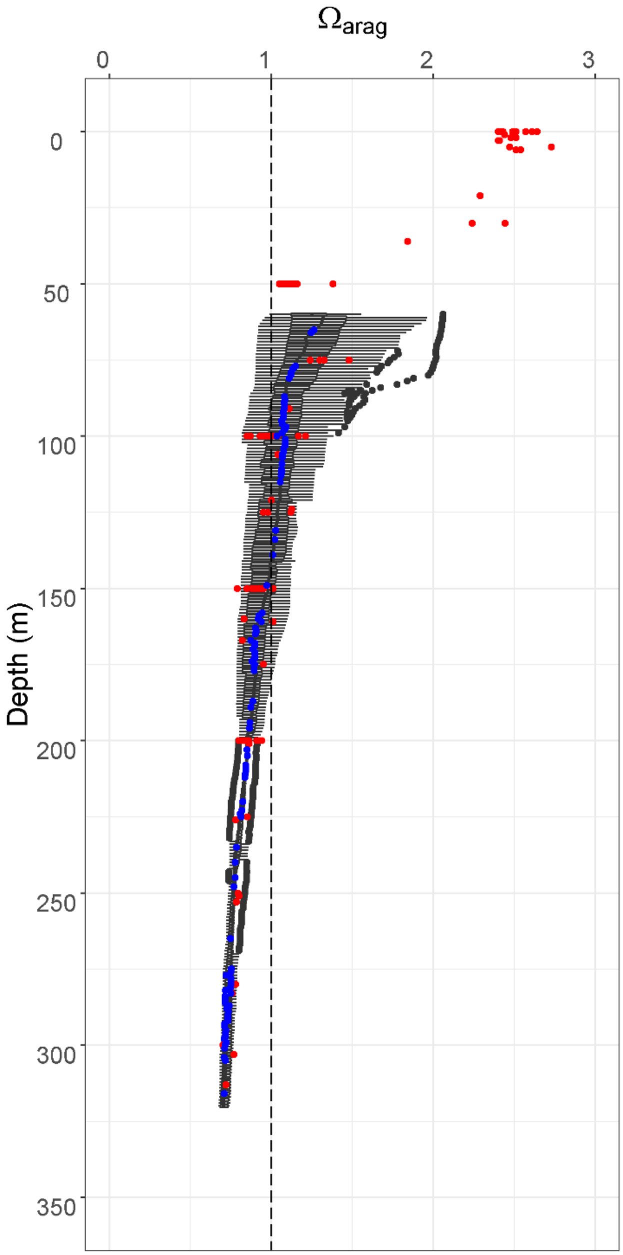

Supplementary materials Figure 3: **Hierarchical levels of *Lophelia pertusa* cold-water corals.** The multiscale material setup of cold-water corals (CWC) ranges from reef framework to aragonite crystals (based on Mass et al. 2014; Mouchi et al. 2017) and illustrates the order of length scales investigated here. Skeletal density was measured on ball-milled dust with particle sizes ~1 µm. EBSD measurements provide results on the aragonite needle length scale. Nanoindentation and Raman was performed on the RAD level while SRµCT imaging was performed at a voxel size of 2.6 µm.

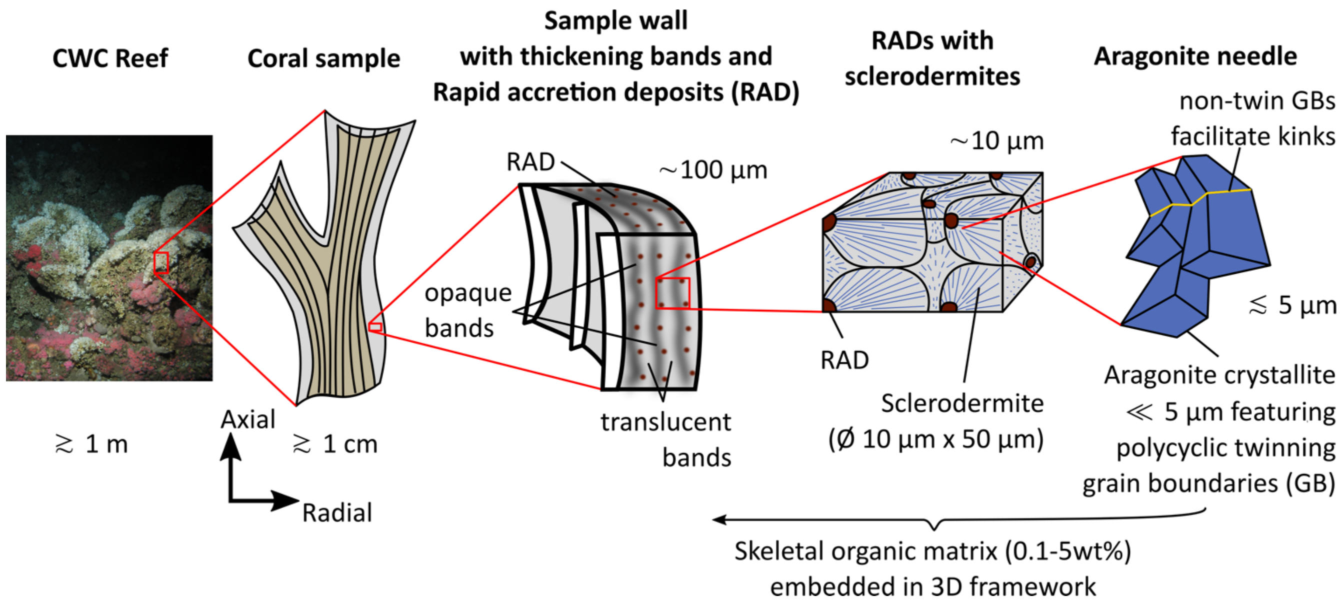

Supplementary materials Figure 4: Density, mechanics and material chemistry of CINMS *L. pertusa.* The Figure shows a) Raman crystallinity as 1/Full Width Half Maximum (1/FWHM); b) Hardness of the skeletal material measured at microscopic length scales; c) Electron Backscatter Diffraction of live coral above and below the ASH (see also Supplementary Materials Figure 9); d) Ductility (the ratio between plastic and total work) of the skeletal material measured at microscopic length scales; data represented as medians with min/max error bars at respective median (large diamond). Significant differences between live and dead samples are indicated by *.

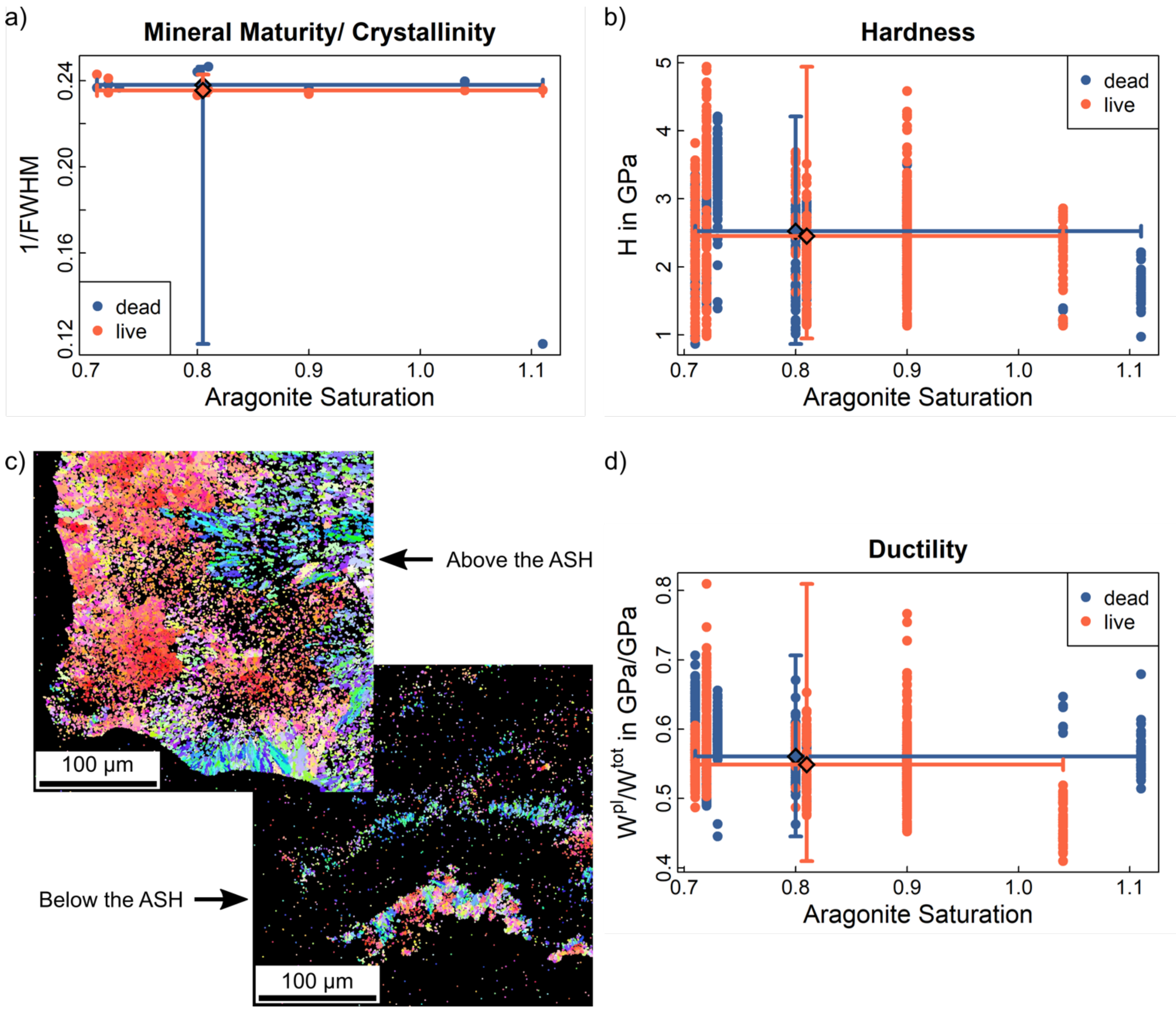

Supplementary materials Figure 5: Image analyses of synchrotron radiation μCT data. a) and b) show cross sections of a dead sample as shown in Figure 4 after converting the data to 16 bit. Images were thresholded and the actual sample volume, white, in c) and d) was determined. To calculate the total, non-porous volume, a binary closing operation was performed to the non-porous volume, white plus blue areas, in c) and d). Volume fraction for the whole polyp was determined by dividing actual volume (white) by total non-porous volume (white + blue). Larger pores, e.g. grey area in (d) due to borers or grown features were not considered by our algorithm. The red arrows in a-d) point to regions were skeletal material was dissolved rather than represented as internal porosity, presumably a later stage in the process. Image processing did not artificially close those spots so that porosity determined is considered internal only and represents a conservative measure.

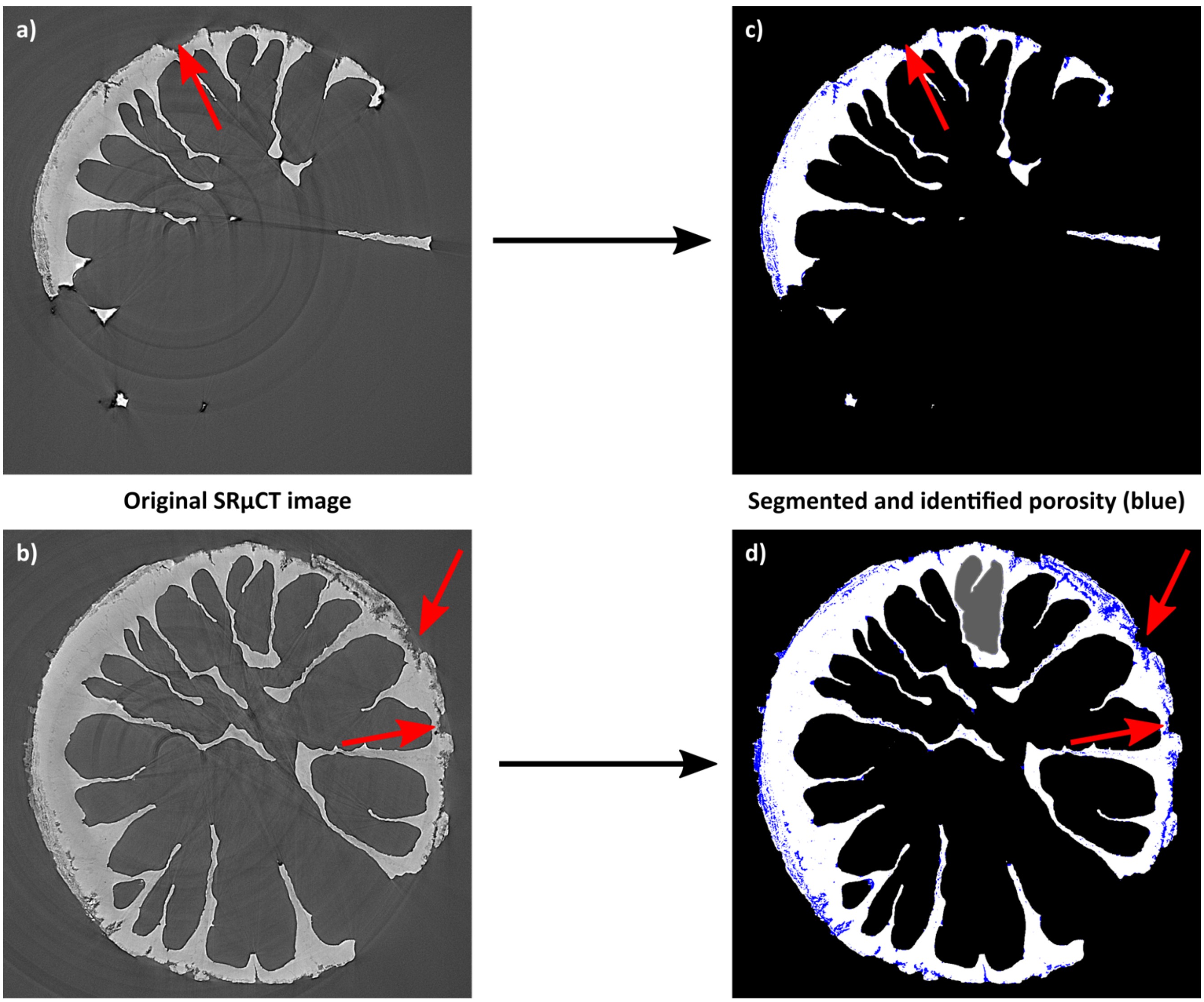

Supplementary materials Figure *6:* a) *Lophelia pertusa* skeleton from above the ASH with (dark) and without soft-tissue (light); b) *L. pertusa* skeleton from below ASH. Line in image (red arrow) indicates where protective soft-tissue was present (right of line) and where there was no protective tissue (left of line), with loss of surface features from dissolution; c) high resolution SEM image of dissolution showing aragonite needles.

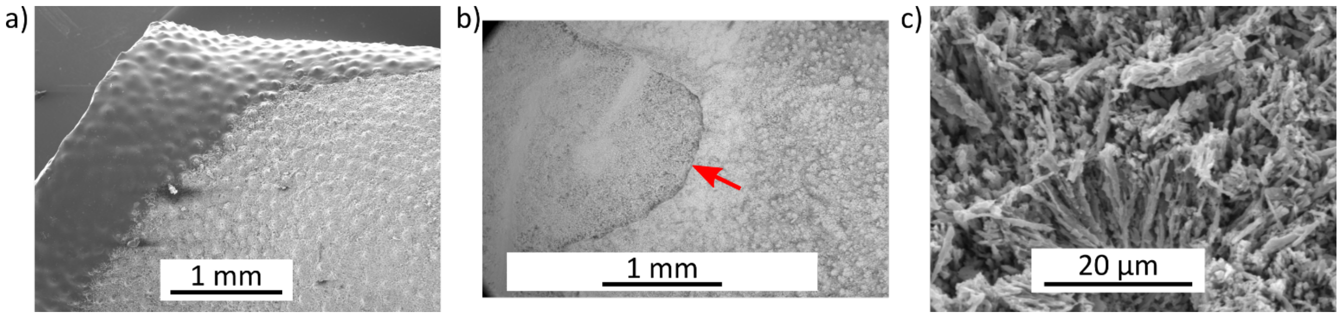

Supplementary materials Figure 7: Skeletal mass density of live and dead *Lophelia pertusa* collected from the Southern California Bight. Image shows median, minimum, and maximum as well as the measured points.

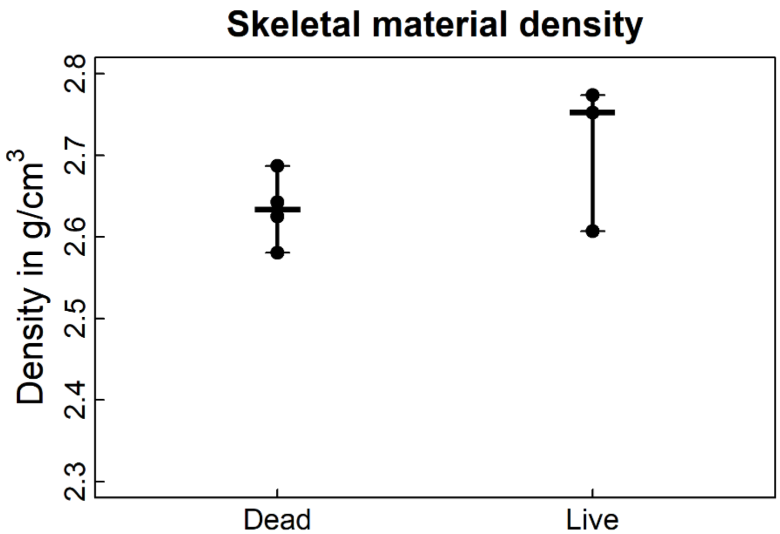

Supplementary materials Figure 8: Scaling up from branch to habitat. Schematic of how the structural integrity model of a hollow cylinder is reproducible and can be expanded through mathematical and computational modelling to create much larger, complex framework. The structural integrity of the framework can then be assessed by integrating information of the exposure to, and severity of the stressor to quantify timescales of habitat crumbling. The shaded area with coral fragments below the coral framework represents coral rubble infilled with sediment, and (…(n)) indicates how the framework can be extended to much larger sizes in a reproducible way. Coral imagery adapted from illustrations by Thompson (1873).

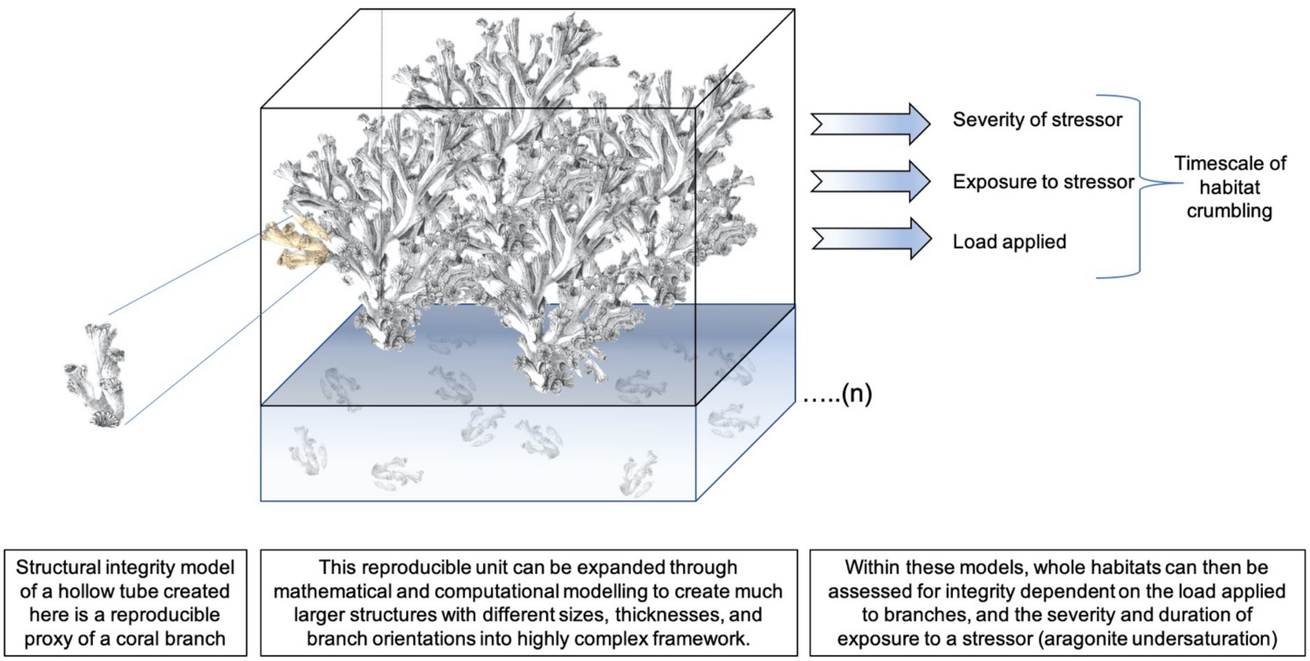

Supplementary materials Figure 9: Electron Backscatter Diffraction (EBSD) of live *Lophelia pertusa* from above and below the aragonite saturation horizon in the Southern California Bight. a) Progression of EBSD processing as scanning electron microscope image (top), aragonite crystal identification (middle) and noise-processed image (bottom). b) EBSD images with pole orientation map of individual aragonite crystals from four different CWC reef sites with different aragonite saturation states ($\mathbf{\Omega}_{arag}$).

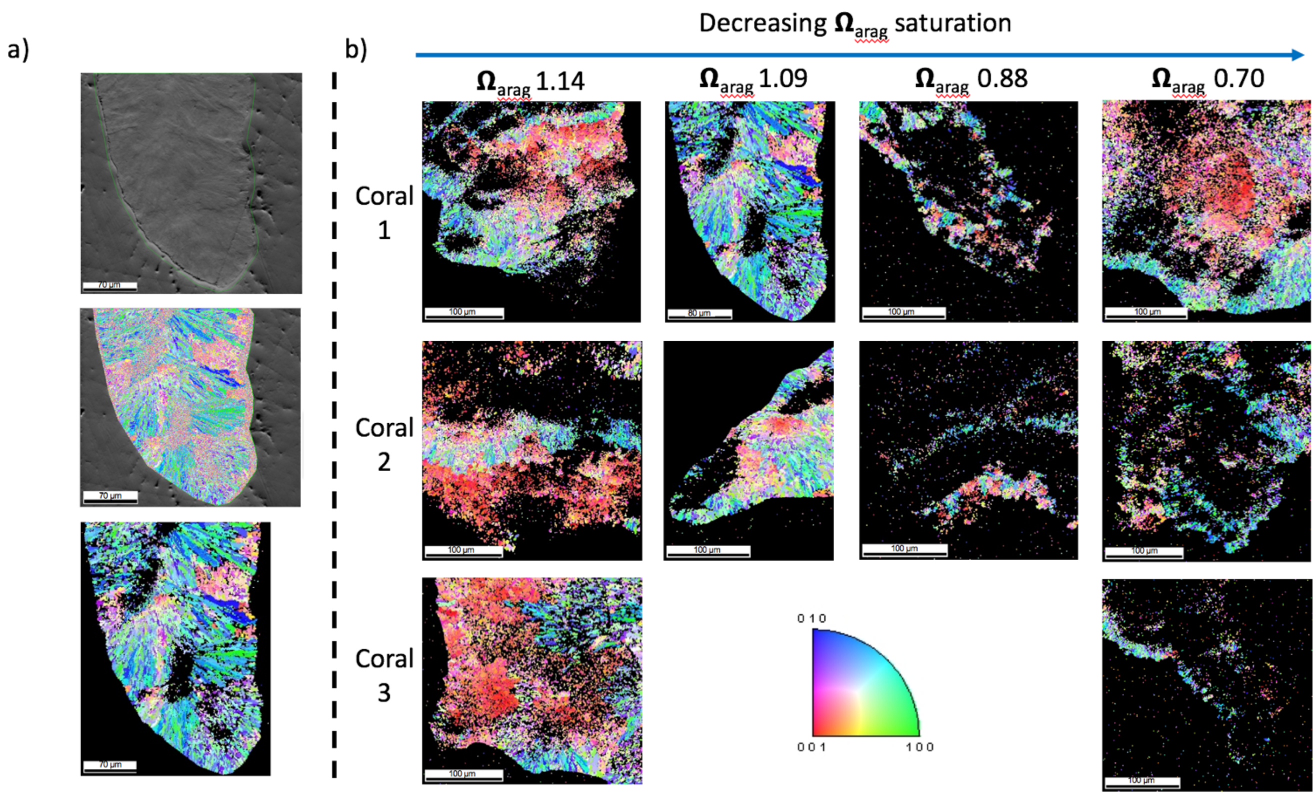

Supplementary materials Figure 10: Two example images of *Lophelia pertusa* in laboratory conditions exhibiting soft-tissue retraction from main skeleton, with full tissue retained in and around corallites. Red arrows indicate line of tissue remaining on skeleton.

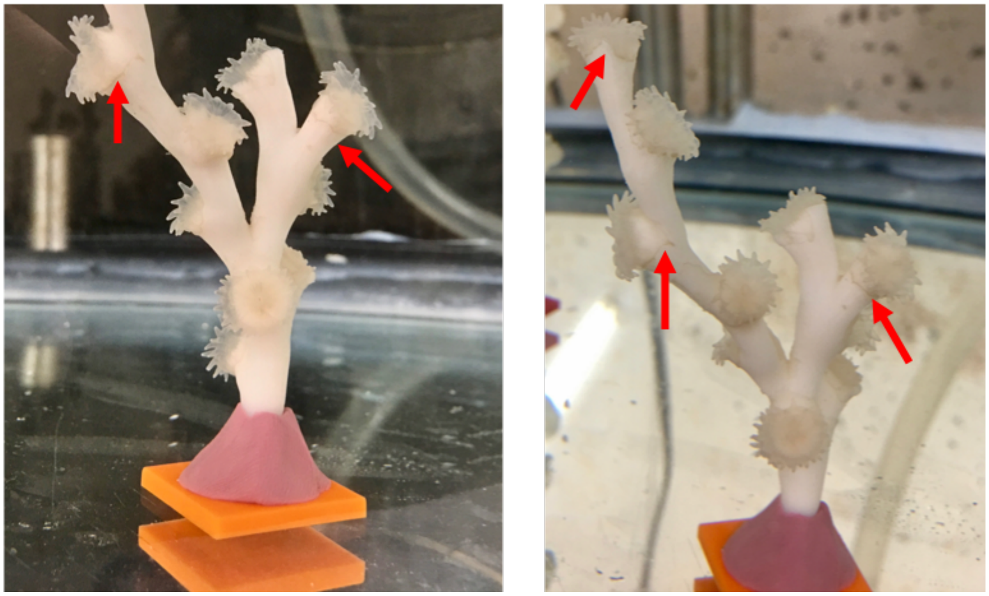

References:

Mass, T., Drake, J.L., Peters, E.C., Jiang, W., and Falkowski, P.G. (2014). Immunolocalization of skeletal matrix proteins in tissue and mineral of the coral *Stylophora pistillata. Proc. Natl. Acad. Sci.* 111, 12728–12733.

Mouchi, V., Vonlanthen, P., Verrecchia, E.P., and Crowley, Q.G. (2017). Multi-scale crystallographic ordering in the cold-water coral *Lophelia pertusa*. *Sci. Rep.* 7, 8987.

Thomson, W.C. (1873). The depths of the Sea. An account of the general results of the dredging cruises of H.M.S. 'Porcupine' and 'Lightning' during the summers 1868, 1869 and 1870. MacMillan and Co., London.